Electronic properties of the MoS_2-WS_2 heterojunction

K. Kośmider[1] and J. Fernández-Rossier[1,2]

[1]*International Iberian Nanotechnology Laboratory (INL), Av. Mestre José Veiga, 4715-330 Braga, Portugal*

[2]*Departamento de Física Aplicada, Universidad de Alicante, 03690 San Vicente del Raspeig, Spain*

(Received 10 December 2012; published 28 February 2013)

We study the electronic structure of a heterojunction made of two monolayers of MoS_2 and WS_2. Our first-principles density functional calculations show that, unlike in the homogeneous bilayers, the heterojunction has an optically active band gap, smaller than the ones of MoS_2 and WS_2 single layers. We find that the optically active states of the maximum valence and minimum conduction bands are localized on opposite monolayers, and thus the lowest energy electron-holes pairs are spatially separated. Our findings portray the MoS_2-WS_2 bilayer as a prototypical example for band-gap engineering of atomically thin two-dimensional semiconducting heterostructures.

DOI: 10.1103/PhysRevB.87.075451 PACS number(s): 73.22.−f

I. INTRODUCTION

Engineering the electronic properties of semiconductors by using heterojunctions has been a central concept in semiconductor science and technology for five decades.[1,2] With the advent of quantum wells, band-gap engineering of quasi-two-dimensional semiconductors made it possible to observe a wealth of new physical phenomena, including the integer and fractional quantum Hall effects in modulation doping GaAs/GaAlAs,[3,4] the condensation of both excitons in double GaAs quantum wells of GaAs,[5] and exciton-polaritons in II-VI quantum wells[6,7] and, more recently, the quantum spin Hall phase in CdTe/HgTe quantum wells.[8]

The isolation[9] of truly two-dimensional crystals, such as graphene and MoS_2, and their use to fabricate field effect transistors,[10,11] has opened a wealth of new venues in physics and material science in general. A particularly interesting possibility is the design of heterostructures formed by a multilayer of weakly coupled two-dimensional crystals.[12] For instance, it is known that the electronic properties of graphene bilayers[13] and graphene deposited on hexagonal boron nitride[14] are different from those of both freestanding graphene and graphene deposited on silicon oxide.

The properties of bulk MoS_2 and its nanostructures, such as nanotubes,[15,16] fullerenes,[17] and nanoislands,[18] have been studied for a long while, including even chemically exfoliated single planes.[19] More recently, the study of electronic and optoelectronic devices based on a single MoS_2 layer has taken the impetus for several reasons. First, it was found that the MoS_2 monolayer exhibits a direct band gap of 1.8 eV with strong photoluminescence,[20,21] as opposed to the indirect gap of 1.29 eV of bulk MoS_2. Second, the fabrication of a high mobility field effect transistor based on a single MoS_2 layer has been reported,[22] showing both the electrical control of transport and optical[23] properties. Third, the combination of graphenelike hexagonal symmetry, large spin-orbit coupling (SOC), and lack of inversion symmetry, give rise to a band structure with two valleys and strong spin-valley coupling.[24] Taking advantage of these unique properties, optical spin pumping is turned into valley-polarized photocarriers,[25–29] which opens new possibilities in the emerging field of valleytronics.[24] In addition, the mechanical properties of MoS_2 have also attracted attention.[30,31]

Importantly, other transition metal dichalcogenides, such as WS_2, as well as $MoSe_2$ and WSe_2 are expected to have similar properties,[32–35] and the first experimental demonstrations of monolayer WS_2 have just been reported.[36] All of the above naturally leads us to investigate the electronic properties of transition metal dichalcogenide (TMD) multilayers.[37–39] Here we report our results on the simplest case, a bilayer of MoS_2 and WS_2, which both have the same crystal structure and very similar lattice constant. In particular we are interested in how the stacking of different TMD monolayers (see Fig. 1) can result in heterostructures with electronic properties different from the homogeneous TMD monolayers and multilayers,

II. METHODS

Our calculations were performed with the Vienna *ab initio* package (VASP),[40] based on the local density-functional approximation,[41] plane-wave basis ($E_{\text{cut}} = 400$ eV), and non-collinear projector-augmented waves (PAW) method.[42,43] The spin-orbit interaction is included using the spherical part of the Kohn-Sham potential inside the PAW spheres as described in Ref. 44. We treat both the transition metal orbitals $4p$, $5s$, $4d$ together with the sulfur orbtials $3s$ and $3p$ as valence states, and the rest are considered as core. We use the Perdew-Burke-Ernzerhof (PBE)[45] version of generalized gradient approximation to describe the exchange-correlation density functional and, in some cases, we also use the hybrid functional in the Heyd-Scuseria-Ernzerhof (HSE)[46] form which is known to give a better description of band gaps in semiconductors. All calculations are carried out using a 1×1 supercell with vacuum thickness not smaller than 17 Å. The BZ is sampled with the Γ-centered Monkhorst-Pack's[47] (MP) meshes of the **k** points. For the PBE calculations the $6 \times 6 \times 1$ mesh is used, whereas for the HSE calculations—due to their high computational cost—the mesh is reduced to $5 \times 5 \times 1$.

III. ELECTRONIC STRUCTURE RESULTS

In this section we present and discuss the results of our DFT calculations for MoS_2 and WS_2 monolayers and their heterostructures. Attention is paid to the value and nature of the band gaps and spin-orbit splittings at the K points. The

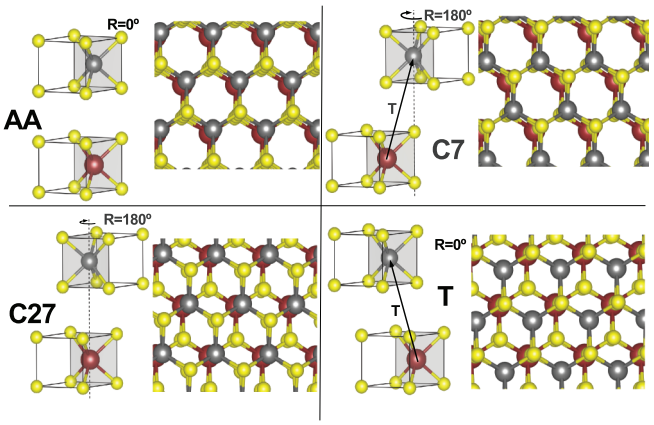

FIG. 1. (Color online) Schematic views of the MoS_2-WS_2 heterojunction of different stacking (i.e., C7, C27, AA, T). Each stacking is obtained either by a monolayers translation T and /or a rotation R with respect to each other. Red, gray, and yellow spheres represent W, Mo, and S atoms, respectively.

influence of the nonlocal exchange is discussed at the end of the section.

A. MoS_2 and WS_2 monolayers

For reference we discuss first the electronic properties of isolated MoS_2 and WS_2 monolayers (MLs).[32–35,48,49] The crystal structure of 2H-MoS_2 (2H-WS_2) consists of two 2D parallel triangular lattices of S atoms separated by the same lattice of Mo (W) atoms translated by 1/3 of the unit-cell diagonal, with lattice constant $a = 3.19$ Å ($a = 3.20$ Å).[32] The corresponding Brillouin zone (BZ) is hexagonal, with two inequivalent K and K' points (valleys). We show the corresponding energy bands in Figs. 2(a) and 2(b), which are in agreement with previous work using the same methodology.[33,34] Both MLs are direct band semiconductors with a maximum valence band

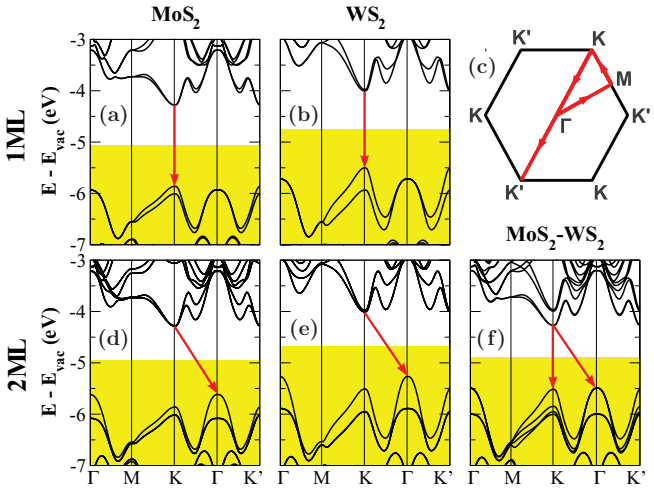

FIG. 2. (Color online) Band structures of (a) MoS_2 monolayer, (b) WS_2 monolayer, (d) MoS_2 bilayer, (e) WS_2 bilayer, and (f) MoS_2-WS_2 heterojunction. The stacking of bilayers is C7 [see Fig. 1(b)]. (c) Scheme of the BZ with the line along which the band structures are calculated. E_{vac} stands for vacuum energy. The Fermi energy lies at the intersection of white and yellow regions.

TABLE I. Band-gap energies E_g (lower values in bold) and spin-orbit splittings Δ_{SOC} of MoS_2, WS_2, and MoS_2-WS_2 systems calculated with the PBE and HSE exchange-correlation energy functionals. The direct (indirect) band gap is calculated between the VB energy at the K (Γ) point and the CB energy at the K point. Slash sign separates Δ_{SOC} values of the MoS_2-WS_2 states localized on the MoS_2 and WS_2 MLs.

		E_g (eV)		Δ_{SOC} (meV)	
		Direct	Indirect	CB	VB
MoS_2	PBE	**1.58**	1.65	3	147
	HSE	**2.01**	2.16	21	202
WS_2	PBE	**1.50**	1.71	27	435
	HSE	**1.90**	2.26	6	577
MoS_2-WS_2	PBE	1.25	**1.22**	3/28	155/414
	HSE	**1.60**	1.68	20/4	214/578

(VB) and minimum conduction band (CB) located in the K and K' valleys. The band-gap values equal 1.58 and 1.50 eV for MoS_2 and WS_2, respectively (see PBE values in Table I). Our calculations also show that, when referred with respect to the vacuum energy, the band structures of both MLs are shifted [cf. Figs. 2(a) with 2(b)], on account of the different electronegativity of the Mo and W.

Because of the lack of inversion symmetry and the strong SOC, the valence and conduction bands are spin split at the K and K' points. The sign of the spin splitting changes from K to K' resulting in the so called strong spin-valley coupling.[24] The splitting is higher in WS_2 ML (435 and 27 meV for VB and CB, respectively) than MoS_2 ML (147 and 3 meV for VB and CB, respectively) due to the higher atomic number of W than Mo.

The band dependence of the spin splittings is accounted for by the atomic orbital composition of the states. Our population analysis reveals that, at the K point, the CB minimum is mostly made by Mo d_{z^2} ($l = 2, m = 0$) orbitals, whereas the VB maximum dominant contribution comes from the d_{xy} and $d_{x^2-y^2}$ ($l = 2, m = \pm 2$) orbitals. To leading order in the SOC, this should yield a nonzero valley dependent spin splitting only in the VB, in agreement with the $\mathbf{k}\cdot\mathbf{p}$ model proposed by Xiao *et al.*[24] However, our calculations show a much smaller, but finite, splitting in the CB at K and K', also reported in previous DFT work,[49] and not captured by the $\mathbf{k}\cdot\mathbf{p}$ model. This interesting issue deserves further theoretical analysis beyond the scope of this work.

B. MoS_2 and WS_2 bilayers

We now discuss the electronic properties of the bilayers that can be formed stacking the WS_2 and MoS_2 monolayers. We have verified that the main features of the electronic structure are quite insensitive to the stacking (see Fig. 1 for the different stackings), thereby we focus on the band structure of the C7 stacking [see Fig. 1(b)] presented in Fig. 2(f). This is the stacking of bulk MoS_2 and WS_2. Comparison of monolayer and bilayer bands in Fig. 2 indicates that interlayer coupling is not strong.

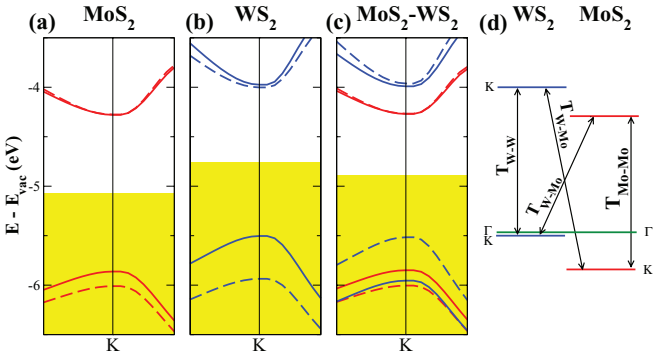

FIG. 3. (Color online) Zoom of band structures at the K point for (a) MoS_2 monolayer, (b) WS_2 monolayer, (c) MoS_2-WS_2 bilayer, and (d) scheme of possible optical transitions in the MoS_2-WS_2 bilayer. Blue (red) lines describe the bands of the states localized on the W (Mo) atoms. Bold (dashed) lines describe the states of spin up (down).

The electronic structure of Mo-Mo and W-W bilayers [Figs. 2(d) and 2(e)] can be rationalized in terms of two concepts: interlayer coupling of degenerate monolayer states, which splits most of the monolayer states, and the existence of a symmetry center in the C7 stacking, which prevents spin splittings. The interlayer splitting is significantly stronger for the valence band at the Γ point than for the VB and CB at K points. As a result, the highest VB state moves to the Γ point for the W-W and Mo-Mo bilayers, which become indirect gap systems.

C. MoS_2-WS_2 heterostructure

In the case of the Mo-W heterojunction the interlayer coupling competes with the energy difference of the monolayer states, shown in Figs. 2(a) and 2(b). As a result, the VB at the Γ point is almost degenerate ($\Delta E_{VB} = 27$ meV) with the top of the VB at the K and K' points. Consequently, a significant population of photoexcited holes will be available at the K and K' points, and photoluminescence will be not quenched. In this sense, the MoS_2-WS_2 heterojunction—unlike the homogeneous bilayers—will be optically active. In addition, the Mo-W bilayer does not have inversion symmetry, so that spin splittings at the K and K' points occur like in the monolayers.

In Fig. 3 we present a summary of the electronic states of the MoS_2, WS_2, and MoS_2-WS_2 crystals in a neighborhood of the K point. These are the relevant states for interband optical experiments. It is apparent that interlayer coupling at this point is negligible and the bilayer bands are nothing but a superposition of the monolayer states. As a result, the top of the VB is in the W layer and the bottom of the CB name lies in the Mo layer, forming a type II structure.[2] In addition, the Mo-W bilayer gap is 1.2 eV, significantly smaller than the gap of the monolayers. In contrast, the top of the VB at the Γ point is delocalized in both planes. The resulting scheme of levels is shown in Fig. 3(d). We expect that intralayer transitions have a stronger quantum yield, on account of their larger electron-hole overlap,[2] but relaxation to the lower energy spatially separated electron-hole pair is expected.

D. Influence of nonlocal exchange

So far all the discussion has been based on results obtained with PBE local exchange functionals. We now address the influence of the nonlocal part of the exchange correlation, focusing on the size and nature of the band gap as well as on the size of the spin splittings at the K point. For that matter, we have computed the electronic structure of the MoS_2, WS_2 monolayers as well as the MoS_2-WS_2 heterostructure using the HSE functional.[46] To reduce computational costs—apart from the MP mesh reduction mentioned in the Methods section—we calculate eigenvalues only for the limited set of **k** points in the BZ (including K and Γ). Table I compares the band-gap values and spin-orbit splittings calculated with the PBE and HSE functionals. As expected from previous work[34] on MoS_2 and WS_2 monolayers, the HSE functional enlarge the MoS_2-WS_2 band-gap value to 1.6 eV. In the case of the heterostructure of MoS_2-WS_2, the HSE functional yields a clearly direct gap, with the top of the valence band being at the K point, 80 meV above the value at the Γ point, supporting even further the electron-hole separation discussed in the previous section.

IV. SUMMARY

In summary, we have studied the electronic properties of the MoS_2-WS_2 system as an example of transition metal dichalcogenide two-dimensional heterostructure. We find that, in contrast to the Mo-Mo and W-W bilayers, the band gap is direct. Additionally we find that the lowest energy electron and highest energy hole states in the optically active K point are localized on different monolayers. In this sense, the Mo-W bilayer forms a type II heterostructure. The combination of band gap engineering in heterojunctions found here, together with the reported electrical control of electronic and optical properties in these systems,[22,23,38,39] hold the promise of a bright future for optospintronics in two-dimensional transition metal dichalcogenides.

ACKNOWLEDGMENTS

We acknowledge J. W. González and F. Delgado for fruitful discussions. This work has been financially supported by MEC-Spain (Grants FIS2010-21883-C02-01, and CONSOLIDER CSD2007-0010) and Generalitat Valenciana, Grant Prometeo 2012-11.

[1] Z. I. Alferov, Rev. Mod. Phys. **73**, 767 (2001).
[2] P. Y. Yu and M. Cardona, *Fundamentals of Semiconductors* (Springer, New York, 1996).
[3] K. Von Klitzing, Rev. Mod. Phys. **58**, 519 (1986).
[4] D. C. Tsui, H. L. Stormer, and A. C. Gossard, Phys. Rev. Lett. **48**, 1559 (1982).

[5]L. V. Butov, A. L. Ivanov, A. Imamoglu, P. B. Littlewood, A. A. Shashkin, V. T. Dolgopolov, K. L. Campman, and A. C. Gossard, Phys. Rev. Lett. **86**, 5608 (2001).
[6]M. Saba, C. Ciuti, J. Bloch *et al*., Nature (London) **214**, 731 (2001).
[7]H. Deng, G. Weihs, C. Santori *et al*., Science **298**, 199 (2002).
[8]M. König, S. Wiedmann, C. Brune, A. Roth, H. Buhmann, L. W. Molenkamp, X. L. Qi, and S. C. Zhang, Science **318**, 766 (2007).
[9]K. S. Novoselov, D. Jiang, F. Schedin, T. J. Booth, V. V. Khotkevich, S. V. Morozov, and A. K. Geim, Proc. Natl. Acad. Sci. **102**, 10451 (2005).
[10]K. S. Novoselov *et al*., Nature (London) **438**, 197 (2005).
[11]Y. Zhang *et al*., Nature (London) **438**, 201 (2005).
[12]K. S. Novoselov and A. H. Castro Neto, Phys. Scr., T **146**, 014006 (2012).
[13]K. S. Novoselov, E. McCann, and S. V. Morozov *et al*., Nat. Phys. **2**, 177 (2006).
[14]C. R. Dean *et al*., Nat. Nanotech. **5**, 722 (2010).
[15]M. Remskar, A. Mrzel, Z. Skraba, A. Jesih, M. Ceh, J. Demar, P. Stadelmann, F. Lvy, and D. Mihailovic, Science **292**, 479 (2001).
[16]A. N. Enyashin, L. Yadgarov, L. Houben, I. Popov, M. Weidenbach, R. Tenne, M. Bar-Sadan, and G. Seifert, J. Phys. Chem. C **115**, 24586 (2011).
[17]F. L. Deepak, H. Cohen, S. Cohen, Y. Feldman, R. Popovitz-Biro, D. Azulay, O. Millo, and R. Tenne, J. Am. Chem. Soc. **129**, 12549 (2007).
[18]S. Helveg *et al*., Phys. Rev. Lett. **84**, 951 (2000).
[19]D. Yang, S. J. Sandoval, W. M. R. Divigalpitiya, J. C. Irwin, and R. F. Frindt, Phys. Rev. B **43**, 12053 (1991).
[20]A. Splendiani, L. Sun, Y. Zhang, T. Li, J. Kim, C.-Y. Chim, G. Galli, and F. Wang, Nano Lett. **10**, 1271 (2010).
[21]K. F. Mak, C. Lee, J. Hone, J. Shan, and T. F. Heinz, Phys. Rev. Lett. **105**, 136805 (2010).
[22]B. Radisavljevic, A. Radenovic, J. Brivio, V. Giacometti, and A. Kis, Nat. Nanotech. **6**, 147 (2011).
[23]A. K. M. Newaz, D. Prasai, J. I. Ziegler, D. Caudel, S. Robinson, R. F. Haglun, Jr., and K. I. Bolotin, Solid State Commun. **155**, 49 (2013).
[24]D. Xiao, G. B. Liu, W. Feng, X. Xu, and W. Yao, Phys. Rev. Lett. **108**, 196802 (2012).
[25]T. Cao *et al*., Nat. Commun. **3**, 887 (2012).
[26]H. Zeng, J. Dai, W. Yao, D. Xiao, and X. Cui, Nat. Nanotech. **3**, 490 (2012).
[27]K. F. Mak, K. He, J. Shan, and T. F. Heinz, Nat. Nanotech. **7**, 494 (2012).
[28]G. Sallen, L. Bouet, X. Marie, G. Wang, C. R. Zhu, W. P. Han, Y. Lu, P. H. Tan, T. Amand, B. L. Liu, and B. Urbaszek, Phys. Rev. B **86**, 081301(R) (2012).
[29]Q. Wang, K. Kalantar-Zadeh, A. Kis *et al*., Nat. Nanotech. **7**, 699 (2012).
[30]A. Castellanos-Gomez, M. Poot, G. A. Steele, H. S. J. van der Zant, N. Agrat, and G. Rubio-Bollinger, Adv. Mater. **24**, 772 (2012).
[31]S. Bertolazzi, J. Brivio, and A. Kis, ACS Nano **5**, 9703 (2011).
[32]Z. Y. Zhu, Y. C. Cheng, and U. Schwingenschlögl, Phys. Rev. B **84**, 153402 (2011).
[33]H. Jiang, J. Phys. Chem. C **116**, 7664 (2012).
[34]A. Ramasubramaniam, Phys. Rev. B **86**, 115409 (2012).
[35]W. Feng, Y. Yao, W. Zhu, J. Zhou, W. Yao, and D. Xiao, Phys. Rev. B **86**, 165108 (2012).
[36]H. Gutiérrez *et al*., Nano Lett. (2013), doi: 10.1021/nl3026357.
[37]A. Castellanos-Gomez, E. Cappelluti, R. Roldan, N. Agrait, F. Guinea, and G. Ruibio-Bollinger, Adv. Mater. **25**, 899 (2013).
[38]H. Zeng *et al*., arXiv:1208.5864.
[39]S. Wu *et al*., Nat. Phys. (2013), doi: 10.1038/nphys2524.
[40]G. Kresse and J. Furthmüller, Comput. Mater. Sci. **6**, 15 (1996); Phys. Rev. B **54**, 11169 (1996).
[41]W. Kohn and L. J. Sham, Phys. Rev. **140**, A1133 (1965).
[42]P. E. Blöchl, Phys. Rev. B **50**, 17953 (1994).
[43]D. Hobbs, G. Kresse, and J. Hafner, Phys. Rev. B **62**, 11556 (2000).
[44]Y.-S. Kim, K. Hummer, and G. Kresse, Phys. Rev. B **80**, 035203 (2009).
[45]J. P. Perdew, K. Burke, and M. Ernzerhof, Phys. Rev. Lett. **77**, 3865 (1996).
[46]J. Heyd, G. E. Scuseria, and M. Ernzerhof, J. Chem. Phys. **124**, 219906 (2006).
[47]H. J. Monkhorst and J. D. Pack, Phys. Rev. B **13**, 5188 (1976).
[48]T. Cheiwchanchamnangij and W. R. L. Lambrecht, Phys. Rev. B **85**, 205302 (2012).
[49]E. S. Kadantseva and P. Hawrylak, Solid State Commun. **152**, 909 (2012).